Gain-of-Function Mutations in the MEC-4 DEG/ENaC Sensory Mechanotransduction Channel Alter Gating and Drug Blockade

Austin L. Brown,[1] Silvia M. Fernandez-Illescas,[2] Zhiwen Liao,[2] and Miriam B. Goodman[1,2]

[1]Biophysics Program and [2]Department of Molecular and Cellular Physiology, Stanford University School of Medicine, Stanford, CA 94305

MEC-4 and MEC-10 are the pore-forming subunits of the sensory mechanotransduction complex that mediates touch sensation in *Caenorhabditis elegans* (O'Hagan, R., M. Chalfie, and M.B. Goodman. 2005. *Nat. Neurosci.* 8:43–50). They are members of a large family of ion channel proteins, collectively termed DEG/ENaCs, which are expressed in epithelial cells and neurons. In *Xenopus* oocytes, MEC-4 can assemble into homomeric channels and coassemble with MEC-10 into heteromeric channels (Goodman, M.B., G.G. Ernstrom, D.S. Chelur, R. O'Hagan, C.A. Yao, and M. Chalfie. 2002. *Nature.* 415:1039–1042). To gain insight into the structure–function principles that govern gating and drug block, we analyzed the effect of gain-of-function mutations using a combination of two-electrode voltage clamp, single-channel recording, and outside-out macropatches. We found that mutation of A713, the *d* or degeneration position, to residues larger than cysteine increased macroscopic current, open probability, and open times in homomeric channels, suggesting that bulky residues at this position stabilize open states. Wild-type MEC-10 partially suppressed the effect of such mutations on macroscopic current, suggesting that subunit–subunit interactions regulate open probability. Additional support for this idea is derived from an analysis of macroscopic currents carried by single-mutant and double-mutant heteromeric channels. We also examined blockade by the diuretic amiloride and two related compounds. We found that mutation of A713 to threonine, glycine, or aspartate decreased the affinity of homomeric channels for amiloride. Unlike the increase in open probability, this effect was not related to size of the amino acid side chain, indicating that mutation at this site alters antagonist binding by an independent mechanism. Finally, we present evidence that amiloride block is diffusion limited in DEG/ENaC channels, suggesting that variations in amiloride affinity result from variations in binding energy as opposed to accessibility. We conclude that the *d* position is part of a key region in the channel functionally and structurally, possibly representing the beginning of a pore-forming domain.

The Journal of General Physiology

INTRODUCTION

Classical approaches to probing the relationship between structure and function in ion channels include site-directed mutagenesis of conserved residues, analysis of chimeric channels, and X-ray crystallography. Although structures have been solved for mechanosensitive channels of bacteria (Chang et al., 1998; Bass et al., 2002), no three-dimensional structure is currently available for any eukaryotic mechanosensitive channel, including the MEC-4 channel. Likewise, no structural data are available for any other member of the degenerin and epithelial Na^+ channel (DEG/ENaC) family. MEC-4 is a 768–amino acid protein composed of two transmembrane domains separated by a large extracellular loop (Lai et al., 1996). Residues conserved among members of the DEG/ENaC family include several near the predicted second transmembrane domain, TM2. Structure–function studies using site-directed mutagenesis to modify ENaCs have revealed that several of these conserved residues contribute to gating, ion selectivity, and amiloride blockade (Kellenberger et al., 2002).

Compared with site-directed mutagenesis, which presumes conserved residues are critical for function, genetic screens provide a model-independent approach for identifying residues of functional importance. Genetic screens in *Caenorhabditis elegans* have recovered 10 missense alleles of *mec-4* that affect residues in or near TM2 (Driscoll and Chalfie, 1991; Hong et al., 2000; Royal et al., 2005). One of these alleles, *u2*, replaces a conserved glycine residue with aspartate (Hong et al., 2000) and alters ion selectivity of the native mechanotransduction current (O'Hagan et al., 2005). Three missense alleles, *e1611*, *u231*, and *u56*, replace an alanine at position 713 with valine, threonine, or aspartate, respectively (Driscoll and Chalfie, 1991; Hong et al., 2000). All three mutations cause swelling followed by degeneration of *C. elegans* touch neurons (the Deg phenotype) and concomitant loss of touch sensitivity (the Mec phenotype) when the mutant proteins are overexpressed (Hong et al., 2000). Substitutions (A to V) at the equivalent positions in DEG-1 and MEC-10 produce similar Deg phenotypes (Chalfie and Wolinsky, 1990;

Correspondence to Miriam B. Goodman: mbgoodman@stanford.edu

Abbreviations used in this paper: DEG/ENaC, degenerin and epithelial Na^+ channel; MTSES, (2-sulfonatoethyl) methanethiosulfonate.

Huang and Chalfie, 1994). Because of the degeneration phenotype produced by mutation at this position, it is called the *d* position.

For obvious reasons, the effect of degeneration-causing mutations on MEC-4–dependent channel function cannot be studied using in vivo recording. Nonetheless, genetic studies have provided useful insights into the structural determinants of MEC-4–dependent degeneration in vivo. For example, transgenes encoding MEC-4 with residues larger than alanine at the *d* position cause dominant Mec and Deg phenotypes, while those introducing residues smaller than alanine cause neither dominant Mec nor Deg phenotypes (Driscoll and Chalfie, 1991). Driscoll and Chalfie (1991) proposed that bulky residues prevent channel closure. Because the Mec and Deg phenotypes are only an integrative manifestation of what occurs at the molecular level, however, a genetic approach cannot be used to test this hypothesis or to evaluate whether or not any particular mutation alters additional aspects of channel function, including ion selectivity or single-channel conductance.

MEC-4 is coexpressed with MEC-10 in vivo and both proteins are part of the native sensory mechanotransduction complex in *C. elegans* (O'Hagan et al., 2005). Previously, we showed that oocytes expressing wild-type, heteromeric channels expressed small, amiloride-sensitive currents that increased when the *d* residue was mutated to threonine in MEC-4, but not in MEC-10 (Goodman et al., 2002). We also showed that threonine double mutant channels carried larger currents than MEC-4 single mutants. This result indicated that while mutations in MEC-10 have little effect on their own, such mutations can enhance the effect of mutations in MEC-4.

Within the DEG/ENaC family, alterations in channel function with mutation at the *d* position are not restricted to *C. elegans* family members. Indeed, introducing bulky residues at the *d* position in mammalian ENaC subunits increases current amplitude, open probability, and mean open time (Snyder et al., 2000). Similar manipulations of *Drosophila* and mammalian DEG/ENaCs render inactive channels constitutively active in heterologous cells (for review see Kellenberger and Schild, 2002). The picture that has emerged from these studies is that bulky side chains at the *d* position alter gating in all DEG/ENaC channels through a mechanism in which steric hindrance at the *d* position stabilizes open states. The details of this process in MEC-4–dependent ion channels remain poorly resolved, however.

We show that steady-state open probability, but neither single-channel conductance nor surface expression, increases with side chain volume at the *d* position in homomeric channels expressed in *Xenopus* oocytes. Wild-type MEC-10 partially suppressed the increase in macroscopic current in heteromeric channels. We reasoned that if the nature of the *d* residue shapes the pore, the external vestibule, or both, then mutating this residue could affect sensitivity to open-channel blockers. Amiloride and its derivatives block most, if not all, DEG/ENaC channels, including native mechanoreceptor currents in *C. elegans* (O'Hagan et al., 2005). Because blockade is strongly voltage dependent and decreases the mean open time, it is believed to result from occlusion of the channel pore (Kellenberger and Schild, 2002). We therefore used amiloride and two related compounds (benzamil and benzamadine) to probe for possible structural effects of mutation at the *d* position in homomultimeric MEC-4 channels and heteromultimeric MEC-4/MEC-10 channels expressed in *Xenopus* oocytes.

MATERIALS AND METHODS

Constructs

Constructs encoding full-length, wild-type MEC-4 and MEC-10 were propagated in SMC4 bacteria (American Type Culture Collection accession No. PTA-4084) as previously described (Goodman et al., 2002). Constructs encoding full-length, wild-type MEC-2 were propagated in XL1-Blue. Plasmids encoding mutant MEC-4 and MEC-10 isoforms were derived as follows. A restriction fragment of wild-type protein was subcloned into pBluescript and mutagenized in vitro (QuikChange; Stratagene). The mutated fragment was sequenced and reintroduced into the vector encoding full-length MEC-4 and MEC-10 by restriction digest and ligation. Mutations were at position 713 in MEC-4 and 673 in MEC-10. The mutations studied correspond to A713G, A713C, A713S, A713D, A713T, A713V and A673C, A673D, A673T, A673V in MEC-10. Mutations to T and V reproduce the *mec-4(e1611)* and *mec-4(u231)* alleles, while mutation to D reproduces one of two missense mutations found in *mec-4(u56)* (the other is R601C) (Driscoll and Chalfie, 1991; Hong et al., 2000).

Heterologous Expression

Capped cRNAs were synthesized in vitro using mMESSAGE mMACHINE T7 kit (Ambion) and quantified spectroscopically. *Xenopus laevis* oocytes were isolated and injected with 4–10 ng of each cRNA. Oocytes were maintained at 18°C in modified L-15 medium supplemented with gentamicin (144 μM) and amiloride (300 μM) for 2–9 d.

Electrophysiology: Whole-Cell Recordings

Membrane current was measured by two-electrode voltage-clamp (OC-725C, Warner Instruments, LLC) at room temperature (21–24°C). Electrodes (1–4 MΩ) were fabricated on a horizontal puller (P-97; Sutter Instruments) and filled with 3 M KCl. Analogue signals were filtered at 200 Hz (8-pole Bessel filter) and sampled at 1 kHz. A 60-Hz notch filter was used to minimize line noise. Unless indicated, oocytes were superfused with control saline containing (in mM) Na-gluconate (100), KCl (2), $MgCl_2$ (2), $CaCl_2$ (1) and Na-HEPES (10), adjusted to pH 7.4 with NaOH. Amiloride was diluted from a 0.1 M stock solution in DMSO. The amplitude of amiloride-sensitive current was measured as the difference between current measured at −85 mV in the absence and presence of 300 μM amiloride. Voltage ramps (from −100 to +100 mV in 1 s) were applied in the presence and absence of 300 μM amiloride; the difference current was used to measure reversal potentials.

For selectivity experiments, salines of the following composition (in mM) were used: X-gluconate (100), $MgCl_2$ (2), $CaCl_2$ (1),

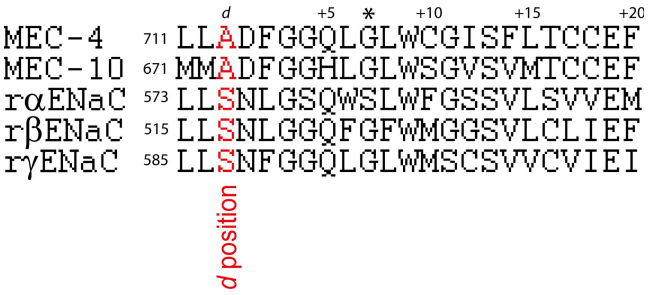

Figure 1. The peri-TM2 domain of MEC-4, MEC-10, and rat ENaCs. The *d* position is highlighted in red. In 267 proteins from 36 species in the DEG/ENaC superfamily, the *d* position is occupied by S > A > G > N in descending order of frequency (Bateman et al., 2004). Residues *n* after the *d* position are labeled *d* + *n* as referenced in the text. Residue *d*+7 is indicated with *; mutations at this position in ENaC decrease amiloride K_i' by ~1,000-fold (Schild et al., 1997).

and NMDG-HEPES (10), adjusted to pH 7.4 with NMDG. Cation X^+ was Na^+, K^+, Li^+, Cs^+, or $NMDG^+$. Sojourns in test solutions were interleaved with control Na^+-gluconate saline to monitor changes in internal Na^+ concentration. Relative permeabilities (P_X/P_{Na}) were calculated using the difference in the reversal potential measured in saline with Na^+ and in solution with X^+ and the Goldman-Hodgkin-Katz voltage equation.

For experiments measuring antagonist affinity, whole-cell currents were measured at voltages between −100 mV and +40 mV in control saline containing different concentrations of antagonist. At least eight concentrations were applied in each recording. Measured current was normalized to the total amiloride-sensitive current. The apparent K_i' was determined by fitting the data according to $I/I_0 = K_i'/(K_i' + [\text{Antagonist}])$, where I_0 is the total antagonist-sensitive current.

An estimate of the electrical depth of the antagonist-binding site within the channel was obtained by fitting a plot of K_i' vs. voltage with Woodhull's model of the voltage dependence of ionic blockade (Woodhull, 1973): $K_i'(V) = K_i'(0)*\exp(z\delta FV/RT)$, where $K_i'(V)$ is the antagonist K_i' at a given voltage V, $K_i'(0)$ is the K_i' in the absence of an electric field, δ is the fraction of the membrane potential acting on the binding site, and z, F, R, and T have their usual meanings.

Electrophysiology: Outside-Out Patches

Vitelline membranes were removed from oocytes manually following incubation in a hypertonic solution composed of (in mM) NMDG-aspartate (220), $MgCl_2$ (1), EGTA (10), KCl (2), HEPES (10), and amiloride (0.3), adjusted to pH 7.4 with NMDG. Pipettes (1.5–3.5 MΩ) were filled with a low-calcium saline solution containing (in mM) Na-gluconate (100), NaCl (2), $CaCl_2$ (2), Na EGTA (5) and HEPES (10), adjusted to pH 7.4 with NaOH. Single-channel and macropatch currents were recorded in an outside-out configuration with a patch-clamp amplifier (WPC-100 E.S.F.; Bioscience Tools), filtered (F_c = 1–5 kHz, 4-pole Bessel filter), and digitized at a rate that was at least three times the filtering frequency. Pulse/Pulsefit software (HEKA Electronics Inc.) was used to control data acquisition; Igor Pro (Wavemetrics) and QuB Software (The Research Foundation of the State University of New York; http://www.qub.ubuffalo.edu) were used for single-channel data analysis. Single-channel conductance and open probability were calculated from all-points histograms derived from leak-subtracted records that were 6 min long on average. Leak currents were estimated by fitting a line to time intervals in which all channels were closed and subtracting the result from

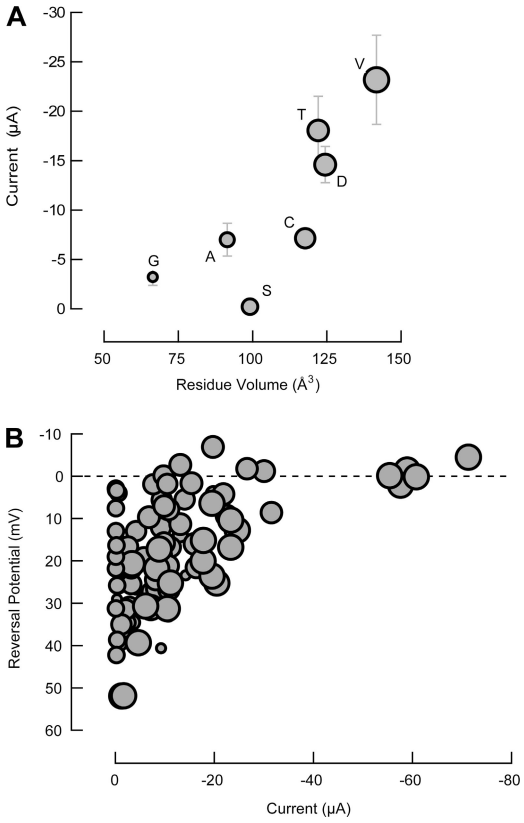

Figure 2. Macroscopic amiloride-sensitive current carried by A713X isoforms. (A) Current amplitude vs. side chain volume at the *d* position. Current was measured at −85 mV. $F(6,109)$ = 8.226, P = 2.38e−07. (B) Current amplitude at −85 mV vs. reversal potential. The reversal potential was measured from amiloride-sensitive *I-V* curves derived from voltage ramps. We recorded from at least seven cells harvested from at least two frogs for all isoforms. Marker size is proportional to side chain volume in A and B.

the data. To minimize line noise, some analogue single-channel records were digitized after conditioning with a 60-Hz noise cancellation device (Humbug; Automate Scientific). We tested whether such conditioning altered measurements of single-channel current, the number of events detected using QuB, or their average dwell times by analyzing conditioned and raw versions of the same record. This analysis showed that none of these parameters differed by >1%. At least 13,000 events were analyzed for each isoform.

Fast Solution Exchange

Solution switching was accomplished using a 16-channel microfluidic chip mounted on a motorized x-y stage (Dynaflow; Cellectricon). Switching times were measured by monitoring the change in liquid junction potential produced by solution exchange. Solution exchange occurred with an exponential time course whose time constant was 1.3 ± 0.6 ms (n = 11 pipettes) when the solution flow rate was 70 nl/s/channel and the stage was moved at maximum speed (30 mm/s).

Reagents

All chemicals were obtained from Sigma-Aldrich. Benzamil and amiloride were diluted from 0.1 M stock solutions in DMSO; benzamidine was diluted from a 1 M stock solution in water.

Statistics and Curve Fitting

Average values are reported as mean ± SEM. Significance was tested using Student's *t* tests or one-way ANOVA followed by posthoc comparisons to data for A713wt channels. ANOVA results are expressed in the form $F(a,b) = c$, where a and b are the degrees of freedom in the ANOVA and c is the value of the F statistic. Curves were fit by a nonlinear least squares method (IgorPro; WaveMetrics); the standard deviation measured at each point was used as a weighting function. The standard error of the coupling energy, $RT\ln\Omega$, was calculated by propagating the errors of the individual K_i' measurements.

Online Supplemental Material

Two tables are provided as supplemental material (available at http://www.jgp.org/cgi/content/full/jgp.200609672/DC1) to the double mutant cycle analysis. Table S1 contains amiloride K_i' values and parameters derived from fitting K_i' vs. voltage plots with the Woodhull equation for all combinations studied. Table S2 contains the results of one-way ANOVA of the K_i' measurements at two voltages.

RESULTS

The Domain that Includes the *d* Position in DEG/ENaC Proteins Is Highly Conserved

The ASC protein family from Pfam (Bateman et al., 2004) includes *C. elegans* degenerins and ENaC channel proteins from nematodes, insects, mammals, amphibians, and fish. Across these diverse metazoan species, the *d* position, which can mutate to cause degeneration in *C. elegans*, is occupied by serine, alanine, glycine, or asparagine in descending order of frequency (Fig. 1). Introducing bulky residues at this position (residue 713 in MEC-4) renders MEC-4 channels constitutively active (Goodman et al., 2002), suggesting that substitutions at the *d* position alter gating. To explore this idea further and to understand the mechanistic basis for changes in gating, we compared the function of wild-type and mutant MEC-4 homomeric channel isoforms expressed in *Xenopus* oocytes. We focused our analysis on amino acid substitutions that reproduce common wild-type alleles in other family members (G, S), introduce a site for covalent modification (C), or reproduce mutant alleles that cause degeneration in vivo (V, T, D). To enhance current amplitude, all channel isoforms were coexpressed with MEC-2 (Goodman et al., 2002).

Amplitude and Relative Permeability of A713X Isoforms

On average, amiloride-sensitive current increased with the volume of the amino acid residue at the *d* position (Fig. 2). Because expressing DEG/ENaC channels in *Xenopus* oocytes can increase cytoplasmic Na^+ concentrations (Canessa et al., 1994; Goodman et al., 2002), we incubated oocytes in culture medium containing 300 μM amiloride. To determine whether this maneuver was successful in preventing Na^+ loading, we measured the reversal potential of amiloride-sensitive current. The reversal potential expected if amiloride-sensitive currents are carried only by Na^+ was calculated from the Nernst potential, $E_{rev} = (RT/zF)\ln[Na^+]_o/[Na^+]_i$. Assuming that channel expression has no effect on internal Na^+ concentration and that the internal Na^+ concentration is 22 mM, as reported for one-celled *Xenopus* embryos (Gillespie, 1983), $E_{rev} \approx +41$ mV in our solutions. We found that amiloride-sensitive currents reversed polarity near +40 mV in cells expressing small currents, but that currents reversed polarity near 0 mV in cells expressing large currents (Fig. 2). This trend was evident for all MEC-4 isoforms examined except for A713S. (Currents in cells expressing A713S were too small to measure and this isoform was not analyzed further.) Thus, channel expression can alter internal Na^+ concentration, and the extent of Na^+ loading is proportional to the amplitude of the amiloride-sensitive current expressed by each cell.

Variation in current amplitude might also derive from mutation-induced changes in relative ionic permeability. The permeability for Li^+, K^+, Cs^+, and $NMDG^+$ relative to Na^+, P_x/P_{Na}, was similar for all MEC-4 isoforms tested. As reported previously for A713T (Goodman et al., 2002), we found $P_{Li} > P_{Na} > P_K > P_{Cs} > P_{NMDG}$ (Table I). Thus, mutating the *d* residue does not affect ion selectivity.

TABLE I

Relative Permeability for A713X Homomeric Channels

Isoform	P_{Li}	P_K	P_{Cs}	P_{NMDG}
A713wt	1.30 ± 0.04 (5)	0.24 ± 0.02 (5)	0.14 ± 0.01 (5)	0.20 ± 0.02 (5)
A713G	1.45 ± 0.07 (6)	0.27 ± 0.07 (6)	0.19 ± 0.08 (5)	0.09 ± 0.03 (6)
A713C	1.19 ± 0.02 (5)	0.34 ± 0.07 (5)	0.19 ± 0.03 (5)	0.12 ± 0.02 (5)
A713T[b]	1.44 ± 0.04 (19)	0.17 ± 0.02 (21)	0.044 ± 0.003 (14)	0.0140 ± 0.0009 (14)
A713D	1.66 ± 0.04 (4)[a]	0.26 ± 0.02 (5)	0.12 ± 0.03 (5)	0.06 ± 0.01 (5)[a]
A713V	1.54 ± 0.08 (5)	0.17 ± 0.02 (5)	0.04 ± 0.01 (5)	0.10 ± 0.04 (5)

Ionic permeability relative to that for Na^+ (P_X/P_{Na}) was measured for indicated isoforms in two-electrode voltage clamp. Values are P_x/P_{Na} and are expressed as mean ± SEM (n). One-way ANOVA for P_x/P_{Na}: P_{Li}, $F(5,38) = 5.852$, P = 0.0004; P_K, $F(5,40) = 2.966$, P = 0.0.0227; P_{Cs}, $F(5,33) = 3.738$; P = 0.0086; P_{NMDG}, $F(5,39) = 5.688$; P = 0.0.0049.

[a]$P < 0.01$; pairwise Dunnet's test with respect to wild type.

[b]Data for A713T are from Goodman et al. (2002).

The Relationship between Side-Chain Volume at 713 and Single-Channel Properties

Prior in vivo analyses and studies of expressed MEC-4 channels suggest, but do not prove, that bulky residues at the *d* position increase open probability P_o. We tested this idea directly by recording from single MEC-4 A713X channels in outside-out patches from *Xenopus* oocytes and found, as predicted, that P_o increased with side-chain volume (Fig. 3 A). Except for A713D, the single-channel conductance, γ, of mutant isoforms was not significantly different than wild type (Fig. 3 B). We obtained an estimate of *N* from the relationship between whole-cell current (*I*), single-channel properties (P_o, γ), and driving force: $N = I/P_o\gamma(V - E_{rev})$. For each whole-cell recording, we measured *I* and E_{rev} and used the average values of P_o and γ to derive an estimate of *N*. Each of the mutant isoforms expressed significantly fewer channels than A713wt (Fig. 3 C), indicating that an increase in surface expression is not responsible for the increase in macroscopic current with mutation to residues larger than alanine. Additional experiments are required to determine how mutations at the *d* position decrease surface expression of MEC-4 channels in oocytes and to determine if this also occurs in vivo.

Each of the MEC-4 isoforms exhibited distinctive single-channel behavior. Fig. 4 shows representative single-channel recordings obtained from outside-out patches. Every patch was exposed to 50 μM amiloride to verify that the channels being studied were bona fide amiloride-sensitive MEC-4 channels. All isoforms exhibited shorter-lived channel openings in the presence of amiloride than in its absence (Fig. 4), consistent with prior work indicating that amiloride is an open channel blocker in ENaC (Palmer and Frindt, 1986; Kellenberger et al., 2003).

A713wt channels opened briefly and exhibited occasional bursts of channel activity. Replacing the wild-type alanine with glycine did not obviously alter steady-state P_o or mean open time (Table II). By contrast, replacing the wild-type alanine with larger residues resulted in higher P_o, longer open times, and shorter closed times (Table II). A single subconductance state was observed in isoforms with residues larger than alanine, as indicated by the appearance of a shoulder in the all-points histograms (Fig. 4). Rarely, we observed events that resembled visits to subconductance states in A713wt and A713G channels. Such events were difficult to resolve, and because they could represent incomplete closures instead of true subconductances they were not analyzed in detail. The model emerging from these results is one in which the stability of open state(s) in MEC-4 channels increases with the volume of the residue at the *d* position, while the stability of the closed state decreases.

Transitions to the intermediate subconductance state were observed from the both the closed and fully open state for isoforms with residues larger than alanine. Indeed, for A713T, A713D, and A713V isoforms, channels often chattered between the two substates (Fig. 4). For all patches in which substates were detected, the conductance of the larger state was not an integer multiple of the smaller one. Additionally, the relative amplitudes

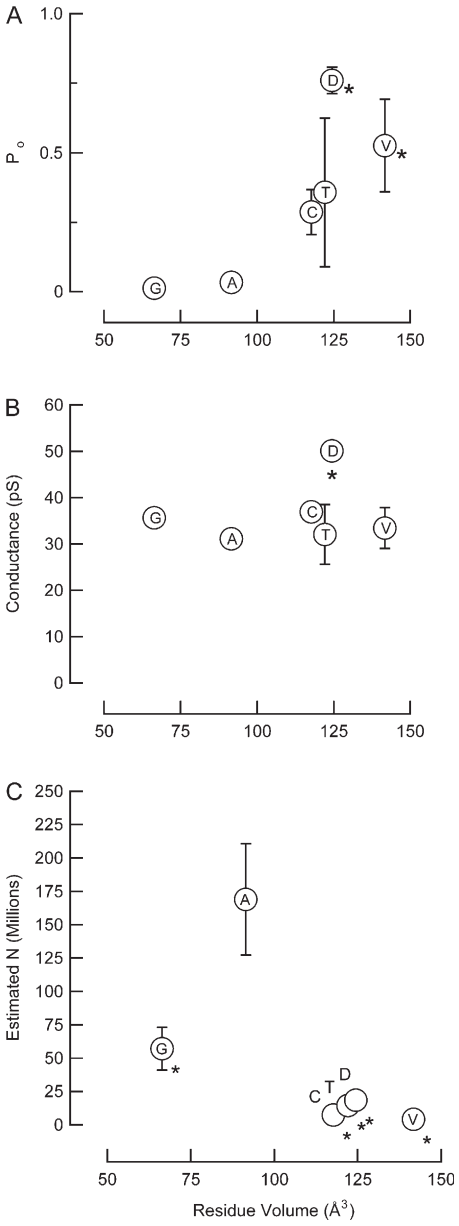

Figure 3. Steady-state open probability, P_o (A), single-channel conductance, γ (B), and estimated channel number, *N* (C), as a function of side-chain volume. Microscopic parameters, P_o and γ, were determined from outside-out patches containing one to two channels. The square root of the probability of not being closed was used as an estimate of P_o for two-channel patches. *N* was estimated as described in the Results. The data are summarized in Table II. One-way ANOVAs for P_o, γ, and *N* were as follows: $F(5,46) = 8.354$, $P = 1.11e\text{-}05$; $F(5,46) = 6.791$, $P = 8.12e\text{-}05$; and $F(5, 97) = 12.94$, $P = 1.2e\text{-}09$. Pairwise Dunnet's test with respect to wild-type: *, $P < 0.01$.

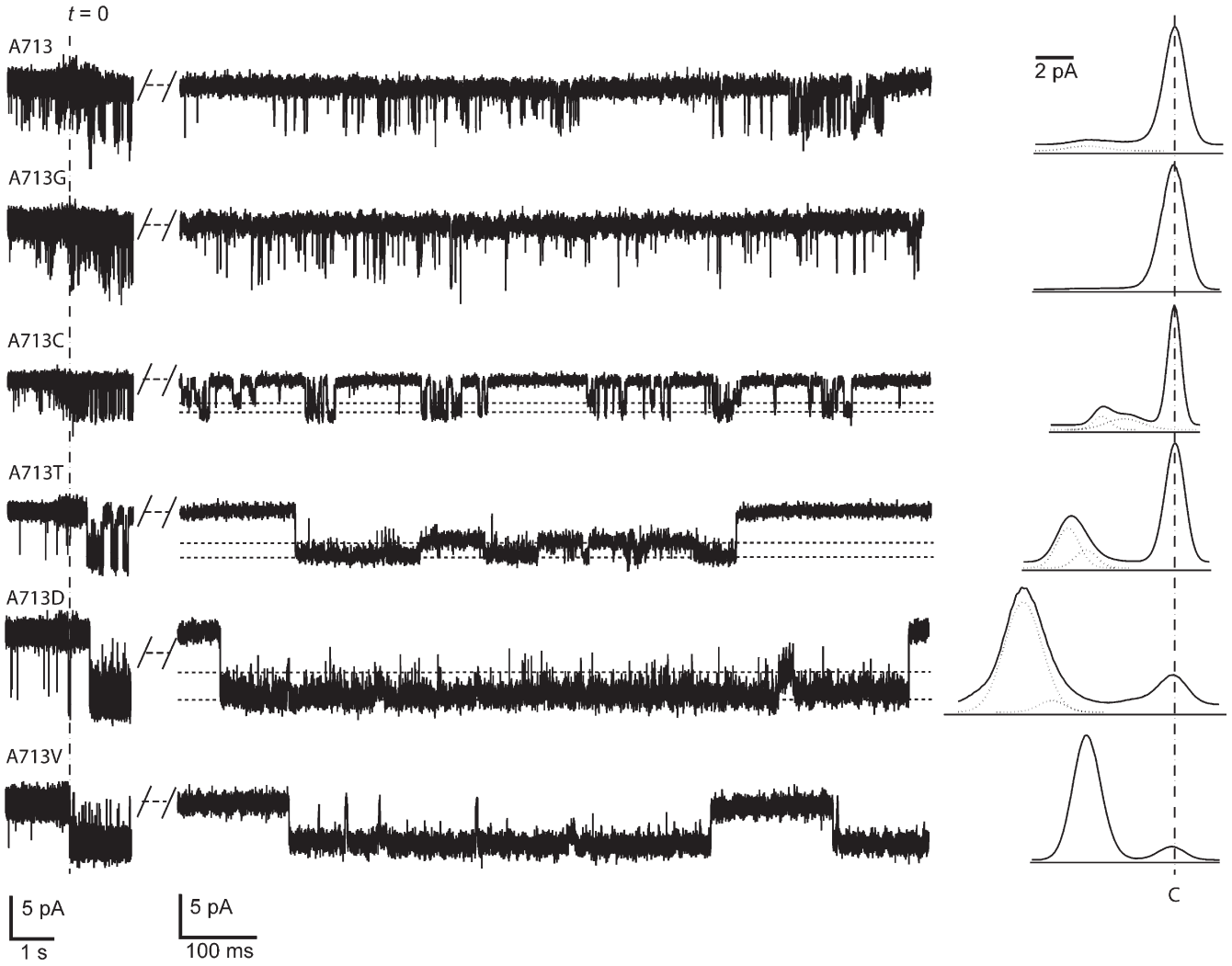

Figure 4. Single-channel recordings of A713X isoforms at −150 mV. Inward current is down and substates are indicated by a horizontal dashed line. To the left of each trace is a segment of the same recording (displayed on a compressed timescale) showing current in the presence ($t < 0$) and absence ($t > 0$) of 50 μM amiloride. All-points histograms are to the right of each trace, including fits to the distribution with a sum of Gaussians. The peak corresponding to the closed state is indicated by the vertical dashed line. Similar results were obtained in at least four patches for each isoform.

of the substates were similar for all isoforms in which substates were detected (Table II). Thus, these events represent sojourns in a true subconductance state. Although the functional significance of substates is not clear, their existence shows that MEC-4 channels can adopt at least two stable open (conducting) states.

In mammalian DEG/ENaC channels that carry a cysteine residue at the *d* position, application of MTS reagents appears to lock channels in an open state (Adams et al., 1998; Kellenberger et al., 2002). We applied (2-sulfonatoethyl) methanethiosulfonate (MTSES) to outside-out patches containing A713C channels, but were not able to resolve any effects at the single-channel level. This failure was not due to inaccessibility of the *d* position, however. Indeed, we found that MTSES increased macroscopic current carried by A713C, but not A713T channels. Before and after MTSES, amiloride-sensitive current at −85 mV was −4.15 ± 1.3 μA and −6.80 ± 1.8 μA ($P < 0.005$, paired Student's *t* test) in six cells expressing A713C channels and −10.5 ± 3.4 μA and −8.95 ± 3 μA ($P = 0.26$, paired Student's *t* test) in four cells expressing A713T channels.

Certain A713X Isoforms Alter Block by Amiloride and Benzamil

Amiloride blocks all DEG/ENaC channels with submicromolar affinity and inhibits current by occluding the permeation pathway. Different isoforms vary in their affinity and in the voltage dependence of blockade (Kellenberger and Schild, 2002). We compared amiloride sensitivity among A713X isoforms at voltages between −100 and +40 mV and found that steady-state

TABLE II

Single-Channel Properties of A713X Homomeric Channels

	γ_1	γ_2	γ_2/γ_1	$<\gamma>$	P_o	τ_o	τ_c
	pS	*pS*		*pS*		*ms*	*ms*
A713wt	ND	31 ± 1 (12)	ND	ND	0.034 ± 0.017 (12)	0.9 ± 0.3 (7)	125 ± 62 (4)
A713G	ND	36 ± 2 (7)	ND	ND	0.014 ± 0.009 (7)	1.2 ± 0.3 (6)	208 (2)
A713C	28 ± 2 (6)	36 ± 2 (16)	1.4 ± 0.1 (6)	35 ± 4 (5)	0.29 ± 0.08 (16)	40 ± 20 (8)	35 ± 15 (6)
A713T	27 ± 4 (3)	38 (2)	1.2 (2)	37 (2)	0.36 ± 0.27 (3)	144 ± 72 (3)	9.3 (1)
A713D	41 ± 2 (4)	50 ± 2 (4)	1.22 ± 0.03 (4)	48 ± 2 (4)	0.76 ± 0.05 (4)	109 ± 47 (3)	21 (1)
A713V	17 ± 6 (3)	35 ± 4 (6)	2.4 ± 1 (3)	23 ± 6 (3)	0.53 ± 0.17 (6)	69 ± 31 (5)	59 ± 21 (4)

Properties of A713X channels measured in outside-out patches from *Xenopus* oocytes. Values are mean ± SEM (n = number of patches). For each isoform, a subset of the collected patches were used for each calculation. Only patches with one to two channels were used to measure γ, P_o, and τ_o. Only patches where no double openings were observed were used to calculate τ_c. γ_1 and γ_2 represent the smaller and larger subconductance state, respectively. For two-channel patches, the square root of the probability of not being closed was used as an estimate of P_o. In cases in which channels lacked substates, the conductance was considered to represent the substate with the closest conductance. $<\gamma>$ represents weighted average conductance calculated according to the relative occupancy of γ_1 and γ_2: $(P_1\gamma_1 + P_2\gamma_2)/(P_1 + P_2)$. Single-channel conductance and P_o were calculated from all-points histograms, which were derived from recordings that were a total of 68.0, 9.4, 91.5, 40.5, 40.4, 23.4 min long for A713wt, A713G, A713C, A713T, A713D, A713V, respectively. Dwell times were derived from recordings containing a total of 69.2, 103.6, 106.8, 17.5, 13.0, 14.0 thousand events for A713wt, A713G, A713C, A713T, A713D, A713V, respectively.

dose–response curves for all isoforms were fit by a single-site binding curve (Fig. 5 A and Table III). Three isoforms, A713G, A713T, and A713D, had reduced affinity for amiloride compared with A713wt (Fig. 5 B). Though the effect on K_i' was modest (2.8-fold, on average), it persisted across the entire voltage range studied (Fig. 5 C). There was no detectable change in the voltage dependence of blockade, however, indicating that mutation did not alter the position of the amiloride-binding site with respect to the electric field. The amiloride K_i' and voltage dependence of block for the A713C and A713V isoforms were similar to those of A713wt (Fig. 5 C and Table III).

Increases in macroscopic amiloride K_i' were not obviously correlated with side-chain volume, polarity, hydrophobicity, or charge of the residue at the *d* position. We probed these observations further by comparing the amiloride K_i' of unmodified A713C channels with that of MTSES-modified channels. Though MTSES increased the average current amplitude (see above) and decreased the voltage dependence of binding, the amiloride K_i' of modified channels was not significantly different than that of unmodified channels at −60 mV (Table III). Thus, changes in amiloride affinity are unlikely to result from differences in side-chain volume or charge alone.

To determine whether mutations at the *d* position alter sensitivity to related compounds, we compared the sensitivity of A713wt and A713T channels to benzamil and benzamidine. Benzamil is an amiloride derivative that contains a benzyl substitution on the guanidinium moiety, while benzamadine is a phenyl-substituted guanidinium ion (Fig. 5 C). Benzamil, like amiloride, is likely to bind in the channel pore since blockade of both A713wt and A713T channels was voltage dependent (Table III). As found for amiloride blockade, A713T channels were less sensitive to benzamil than A713wt (Fig. 5 A). Benzamadine, by contrast, inhibited A713T and A713wt channels with similar affinities at −60 mV, which was significantly lower than that of amiloride and benzamil (Fig. 5 A and Table III). Like amiloride and benzamil, benzamidine blockade was voltage dependent (Fig. 5 C and Table III). The voltage dependence of benzamidine blockade differed between A713wt and A713T channels, however. This suggests that the position of the benzamidine binding site is altered by mutation at the *d* position.

Amiloride and Benzamil Are Open Channel Blockers

Studies of ENaC have shown that amiloride is likely to be an open channel blocker (Palmer and Frindt, 1986; Kellenberger et al., 2003). The simple open state block model

$$C \leftrightarrow B + O \underset{k_{off}}{\overset{[B]k_{on}}{\leftrightarrow}} OB$$

predicts that the on-rate depends linearly on the blocker concentration while the off-rate is concentration independent. To test this model, we measured on- and off-rates for a range of amiloride concentrations (0.5 to 100 μM). Amiloride-supplemented and control salines were applied alternately at 1-s intervals to macropatches held at −60 or −100 mV. The solution switch rate imposed an upper bound (1 ms; see Materials and methods) on the on-rates that could be measured reliably. Accordingly, only concentrations that yielded on-rates $<<1000\ s^{-1}$ were considered. Currents recorded during drug application show that the on-rate increases with concentration, while currents recorded during superfusion with drug-free saline indicate that the off-rate was independent of concentration (Fig. 6 A). At −60 mV,

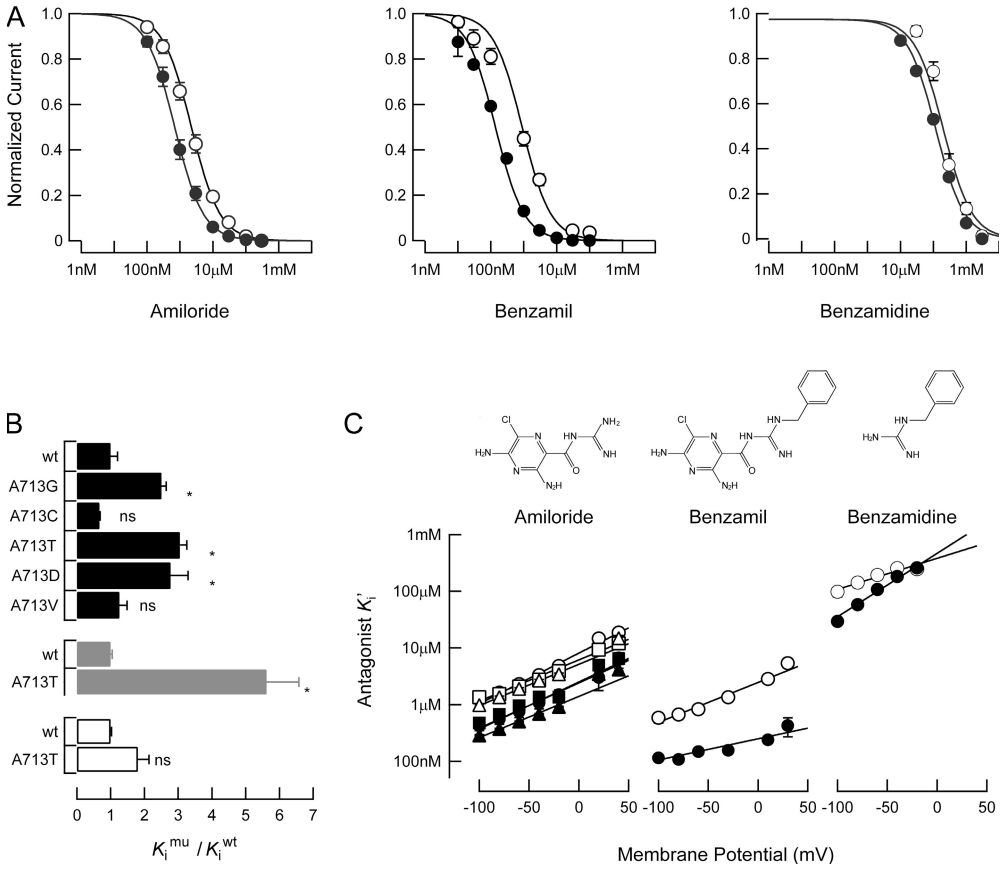

Figure 5. Steady-state blockade by amiloride-related compounds. (A) Normalized dose–response curves at −60 mV for amiloride (left), benzamil (center), and benzamidine (right). Solid and open circles are data for A713wt and A713T channels, respectively. (B) Effect of mutation on K_i' at −60 mV. (C) Antagonist K_i' vs. voltage. Six A713X isoforms were tested for amiloride blockade: solid circles (A713wt), solid squares (A713V), and solid triangles (A713C); open circles (A713T), open squares (A713D), and open triangles (A713G). Curves were fit to the data according to Woodhull's model of voltage-dependent blockade by charged molecules (Woodhull, 1973). See Table II for fitting parameters and the number of oocytes tested for each isoform and compound.

we found that k_{on} was 60 ± 8 $\mu M^{-1}s^{-1}$ and k_{off} was 29 ± 2 s^{-1}.

According to the Woodhull model, charged antagonists that bind externally and do not permeate the pore have on- and off-rates that vary with voltage according to Eqs. 1 and 2, respectively.

$$k_{on}^{'} = k_{on}^{0} \exp(-\delta F \Delta V / 2RT) \quad (1)$$

$$k_{off}^{'} = k_{off}^{0} \exp(\delta F \Delta V / 2RT) \quad (2)$$

In three patches, we compared the rates at holding potentials of −60 and −100 mV. As expected, hyperpolarization increased on-rates and decreased off-rates (Fig. 6 B). At −100 mV we found that k_{on} was 79 ± 2 $\mu M^{-1}s^{-1}$ and k_{off} was 21 ± 1 s^{-1}. Thus, the on-rate increased by a factor of 1.3, while the off-rate decreased by a factor of 1.4. These empirical values are similar to the factor calculated from Eq. 1 and Eq. 2, which was 1.4.

We also compared the on- and off-rates for amiloride to those for the amiloride analogue benzamil. In whole-cell measurements, benzamil blocks A713wt with higher affinity than does amiloride (Fig. 5 and Table II). This affinity difference appears to be due to a much slower off-rate (Fig. 6 B). Interestingly, on-rates for benzamil were also slower (Fig. 6 B). At −60 mV we found that (for benzamil) k_{on} was 17 ± 6 $\mu M^{-1}s^{-1}$ and k_{off} was 4.0 ± 1.1 s^{-1}. Benzamil is expected to have a slower on-rate than amiloride owing to its larger size if on-rates are diffusion limited (see Discussion).

We also measured blocking and unblocking rates for A713T channels. In whole-cell measurements, the affinity for amiloride is reduced by approximately twofold (Fig. 5 and Table II). When we made the analogous measurements in outside-out patches, however, no such difference was observed. This discrepancy was not due to differences in the solutions used to make the measurements (not depicted), but likely reflects a difference in the biophysics of the channel in the two different environments.

Allele-specific Interactions in Mutant MEC-4/MEC-10 Heteromeric Channels

Though MEC-4 is 56% identical to MEC-10, the two proteins are not redundant since loss of *mec-4* alone is sufficient to eliminate mechanoreceptor currents in vivo (O'Hagan et al., 2005). To learn more about how MEC-4 and MEC-10 cooperate to form a single ion channel, we compared macroscopic currents carried by wild-type heteromeric channels to those carried by single- and double-mutant heteromeric channels. In this analysis, we focused on mutating the *d* residue (which is alanine in both MEC-4 and MEC-10) to larger amino acids. We found that mutating the *d* residue to cysteine

TABLE III

Affinity Constants for A713X Homomeric Channels

	K_i' @ −60 mV	K_i' (0 mV)	δ	ΔG°
	μM	*μM*		*kJ/mol*
Amiloride				
A713wt	0.76 ± 0.16 (5)	2.28 ± 0.60	0.47 ± 0.05	−31.9
A713G	1.89 ± 0.10 (6)[a]	6.50 ± 0.56	0.54 ± 0.04	−29.3
A713C	0.51 ± 0.01 (6)	1.86 ± 0.09	0.55 ± 0.01	−32.4
A713T	2.35 ± 0.39 (7)[a]	8.47 ± 0.96	0.53 ± 0.05	−28.6
A713D	2.10 ± 0.15 (8)[a]	6.24 ± 0.36	0.46 ± 0.01	−29.4
A713V	0.95 ± 0.17 (6)	2.96 ± 0.41	0.52 ± 0.01	−31.2
A713C+MTSES	0.59 ± 0.07 (6)	1.51 ± 0.22	0.36 ± 0.03	−32.9
Benzamil				
A713wt	0.15 ± 0.01 (8)	0.28 ± 0.03	0.26 ± 0.06	−37.0
A713T	0.83 ± 0.14 (5)[a]	2.62 ± 0.03	0.56 ± 0.03[b]	−31.5
Benzamidine				
A713wt	108 ± 3 (4)	576 ± 71	0.73 ± 0.01	−18.3
A713T	196 ± 40 (7)	497 ± 87	0.40 ± 0.05[b]	−18.7

Affinity constants, K_i', given as mean ± SEM (*n*). One-way ANOVA for K_i(−60 mV) (excluding A713C channels treated by MTSES): amiloride, $F(5,32) = 12.73$, $P < 1e\text{-}06$; benzamil, $F(1,11) = 39.03$, $P < 0.0001$; benzamidine, $F(1,9) = 3.30$, $P = 0.103$. One way ANOVA for δ: amiloride, $F(5,32) = 1.78$, $P = 0.15$; benzamil, $F(1,11) = 15.04$, $P < 0.005$; benzamidine, $F(1,7) = 19.18$, $P < 0.005$.

[a]$P < 0.01$; pairwise Dunnet's test with respect to wild type in each dataset.

[b]$P < 0.005$; pairwise Dunnet's test with respect to wild type in each dataset.

and aspartate in MEC-4 increased current carried by heteromeric channels, but had little effect in MEC-10 single mutants (Fig. 7 A). Currents carried by valine double mutants were larger than those carried by either single mutant channel (Fig. 7 C), while aspartate and cysteine double mutant channels carried less current than the MEC-4 single mutant (Fig. 7, A and B). Collectively, these observations indicate that mutations at the *d* residue in one subunit influence the effect of mutations in the other and, like allele-specific genetic enhancement and suppression, are consistent with the idea that MEC-4 and MEC-10 interact near the *d* position to regulate channel activity.

To explore this idea further, we measured amiloride K_i' for all of the heteromeric channels studied above. As shown for MEC-4 homomeric channels (Fig. 5 and Table III), mutating the *d* residue to threonine or aspartate in MEC-4 increased amiloride K_i' of hetermomeric channels (Fig. 7 and Table S1; supplemental material available at http://www.jgp.org/cgi/content/full/jgp.200609672/DC1). The effect of mutating MEC-4 on amiloride K_i' depended on whether or not the *d* residue in MEC-10 was also mutant. We quantified the strength of this interaction by treating the dataset as a double mutant cycle. This formalism has been used to define residues in ion channels that interact with both peptide (e.g., Hidalgo and MacKinnon, 1995) and nonpeptide ligands (e.g., Choudhary et al., 2003; Kash et al., 2003). Interacting pairs of amino acid residues are identified based on the following heuristic: if residue *a* interacts with residue *b*, then the effect (on amiloride blockade) of mutating residue *a* should depend on whether or not residue *b* is mutated. If the residues do not interact, then the change in K_i' associated with mutation in MEC-4 is identical to the change in K_i' associated with mutation in MEC-10. We summarized the data by calculating a coupling coefficient, Ω (Hidalgo and MacKinnon, 1995):

$$\Omega = \frac{K_i(wt,wt)\bullet K_i(mu,mu)}{K_i(wt,mu)\bullet K_i(mu,wt)},$$

where *wt* and *mu* indicate wild type and mutant, respectively. If two mutations affect amiloride blockade independently, then Ω will be unity. If the residues interact, then Ω will deviate from unity. The coupling energy was calculated from RTlnΩ.

We found evidence for interaction when the *d* residue was mutated to aspartate and threonine, but not to cysteine or valine. Similar results were found at −100 and −60 mV (Fig. 7, D and E). We verified that measured differences in K_i' were statistically significant using a one-way ANOVA of the values used to calculate Ω and RTlnΩ (see Table S2). Though small (<5 kJ mol^{-1}), coupling energies in heteromeric channels showed an analogous dependence on side-chain identity as that exhibited by homomeric channels (compare Figs. 5 and 7). Other studies have used mutant cycles to infer distances between interacting residues. No such inferences are possible in the present study, however, since residues as close as 4 Å and as distant as 15 Å exhibit coupling energies <5 kJ mol^{-1} (Schreiber and Fersht, 1995). The nonzero coupling energies in aspartate and threonine mutant cycles do suggest, however, that the

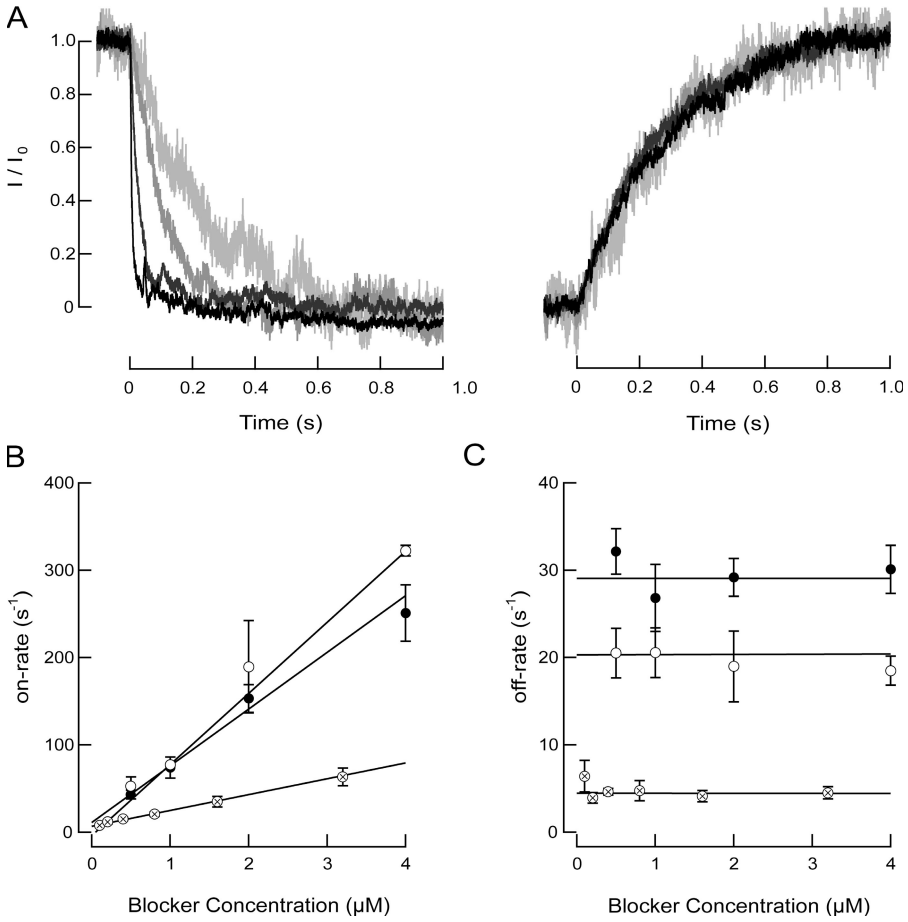

Figure 6. Kinetics of blockade by amiloride-related compounds. (A) Time course of the effect of benzamil on A713wt in outside-out macropatches. $V_h = -60$ mV. Traces corresponding to the effect of 0.1, 0.4, 1.6, and 20 μM benzamil are shown and shaded in proportion to the concentration. (B) On-rates depend on concentration, voltage, and compound. Closed circles are amiloride at $V_h = -60$ mV ($n = 6$), open circles are amiloride at $V_h = -100$ mV ($n = 3$), hatched circles are benzamil at $V_h = -60$ mV. (C) Off-rates depend on voltage and compound, but not concentration. All points are mean ± SEM; lines are fits to averages weighted by the standard deviations.

d residues are close enough to interact with amiloride in the channel pore and imply that the channel pore is unlikely to be wider than the long axis of amiloride (8 Å) near the *d* residue.

DISCUSSION

Large Side Chains at the *d* Position Increase P_o and Mean Open Time

Gain-of-function mutations at the *d* position in *mec-4*, *mec-10*, and *deg-1* cause degeneration in vivo (Chalfie and Wolinsky, 1990; Driscoll and Chalfie, 1991). It was proposed that degeneration occurred in response to unregulated channel activity (Driscoll and Chalfie, 1991). One key tenet of the model is that large residues at the *d* position induce degeneration by increasing the time the channel spends in the open state. We tested this hypothesis by comparing the single-channel properties of gain-of-function mutants known to cause degeneration in vivo to those of mutants that do not. We found that residues that cause degeneration in vivo increase open probability and average open time in homomeric channels and that the extent of this effect increased with side-chain volume. Side-chain charge may also play a role since A713D had the largest open probability (Fig. 3 A). Considered together, our analysis of whole-cell currents, relative ion permeability, and single-channel currents demonstrate that increases in open probability are sufficient to explain the increases in whole-cell current. This finding provides strong support for the idea that introducing large residues at the *d* position favors the open state.

Our data also suggest that the impact of large side chains on P_o depends on subunit–subunit interactions. The following evidence supports this conclusion. Currents carried by mutant homomeric MEC-4 channels were larger than those carried by heteromeric channels composed of mutant MEC-4 and wild-type MEC-10 subunits. This result indicates that wild-type MEC-10 can partially suppress the effect of mutation in MEC-4. Such suppression is not a simple function of the volume of the *d* residue in MEC-4, however, since cysteine single mutant heteromeric channels carried larger currents than valine single mutant heteromeric channels (Fig. 7). We also found that mutating the *d* residue in MEC-10 resulted in either enhancement or suppression depending on the amino acid substitution. These allele-specific interactions suggest a model in which adjacent subunits interact near the *d* position to modify P_o, presumably by altering the stability of the open state.

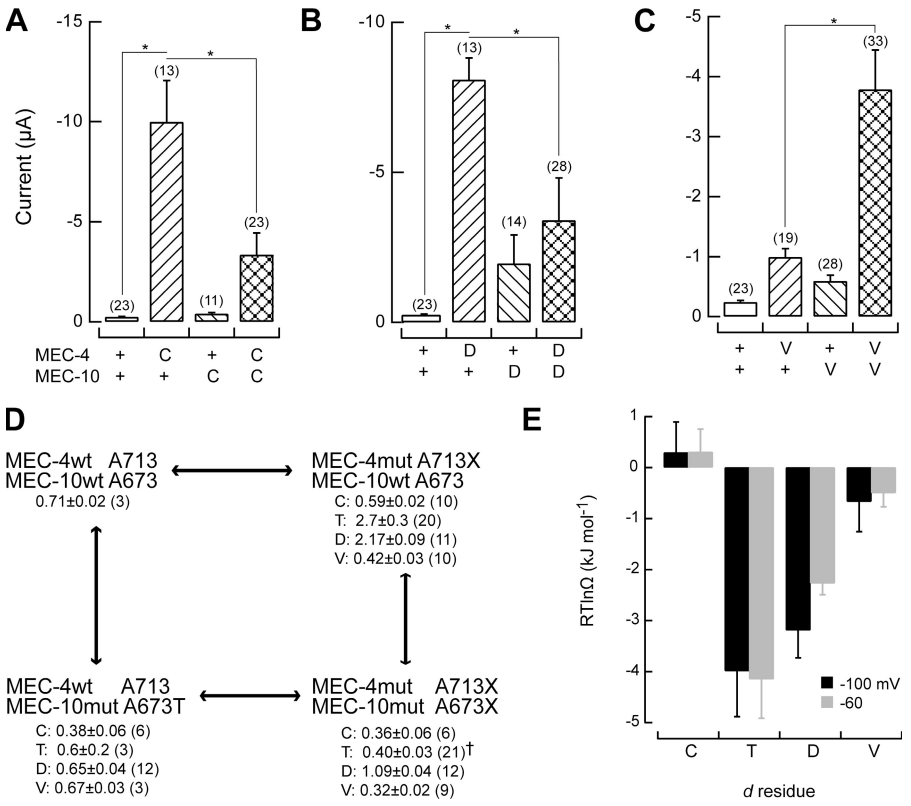

Figure 7. Macroscopic current and amiloride block of MEC-4/MEC-10 heteromultimeric channels. (A) Amiloride-sensitive current in wild type, cysteine single-mutant, and cysteine double-mutant heteromeric channels. (B) Amiloride-sensitive current in wild type, aspartate single-mutant, and aspartate double-mutant heteromeric channels. (C) Amiloride-sensitive current in wild type, valine single-mutant, and valine-double mutant heteromeric channels. In A–C, bars are mean ± SEM for the number of cells indicated above each bar. For ease of comparison, data for wild-type heteromeric channels are repeated in A–C. *, $P < 0.01$, Student's t test for the indicated comparison. (D) Schematic diagram of the mutant cycle, including K_i' measured at −60 mV for each combination. Values are mean ± SEM (in μM) for the number of measurements indicated in parenthesis. (E) Coupling energy, RTlnΩ, for mutations that replace the wild-type alanine with C, T, D, or V in MEC-4 and MEC-10. One-way ANOVA showed that the four K_i values used to calculate each Ω differed from one another at $P < 0.0005$. See Table S1 for K_i' values and Table S2 for full results of the ANOVA. †, data are from Goodman et al. (2002).

Amiloride Blockade Is Likely To Be Diffusion Limited

To determine whether the amiloride binding site is freely accessible in open channels, we sought to compare the measured on-rate constant (k_{on}) to the limit imposed by simple diffusion (k_{diff}). To estimate this limit, we modeled a hemispherical capture domain at the entrance to the pore in order to derive an estimate. In this model, $k_{diff} = 2\pi r_c D N_a$ (adapted from Jones et al., 1998), where r_c is the capture radius, D is the diffusion coefficient, and N_a is Avogadro's number. We defined r_c as the length of amiloride along its long axis (8 Å, measured from PDB 1F5L; Zeslawska et al., 2000) and used a measured value for D, $1.7e{-}6\ cm^2s^{-1}$ (Rabito et al., 1978) to calculate $k_{diff} = 500\ \mu M^{-1}s^{-1}$. It is important to note that this model neglects barriers imposed by membrane surface charges, the need for amiloride to traverse a fraction of the lumen of the pore before reaching its binding site, or the likelihood that amiloride can only bind in a particular orientation. All of these factors would tend to decrease k_{diff}. Indeed, in practice k_{diff} is generally limited to 100 $\mu M^{-1}s^{-1}$ (Hille, 2001).

To evaluate whether or not the measured on-rate is similar to the expected k_{diff}, it is necessary to estimate k_{on} in the absence of applied voltage since the electric field affects k_{on} (Fig. 6 B). We, therefore, derived an estimate of k_{on} at 0 mV from the measured value at −60 mV (Fig. 6 B), the slope factor ($\delta = 0.47$, Table III), and Eq. 1. Using this approach, we find that $k_{on} = 38\ \mu M^{-1}s^{-1}$ at 0 mV. Though this is approximately one order of magnitude slower than the diffusion limit in free solution, it is within a factor of three of the likely practical limit on k_{diff} (see above) and similar to values reported for ENaC (10–30 $\mu M^{-1}s^{-1}$) (Garty and Palmer, 1997).

If amiloride diffusion is rate limiting for block of open channels and if amiloride and benzamil bind in similar ways, then k_{on} should be slower for benzamil because of its larger molal volume. In agreement with this prediction, the measured on-rate constant for benzamil is slower than that of amiloride (Fig. 6 B). Based on the measured voltage dependence of benzamil blockade (Table III), the on-rate for benzamil is 12.4 $\mu M^{-1}s^{-1}$ at 0 mV or approximately one third that of amiloride. We, therefore, propose that diffusion is likely to be rate limiting for block of open MEC-4 and ENaC channels by both amiloride and benzamil.

A Model of How Mutations at the *d* Position Alter Amiloride Blockade

DEG/ENaC channels are not the only proteins known to bind amiloride. Additional targets include proteases such as urokinase-type plasminogen activator or urokinase. Amiloride and related compounds bind urokinase and inhibit its protease function with micromolar

affinity (Vassalli and Belin, 1987). To gain more insight into the difference in affinity for amiloride and benzamidine exhibited by MEC-4 channels, we compared high-resolution (1.8–2.1 Å) 3-D crystal structures of an amiloride-urokinase complex with that of a benzamidine-urokinase complex (Zeslawska et al., 2000). One striking difference in these structures is that at least three additional water molecules are present in the binding pocket when benzamidine is bound compared with when amiloride is bound. This observation raises the possibility that water is displaced when amiloride binds. Release of water molecules upon binding constitutes an entropic factor that could increase the free energy change associated with by as much as ~7 kJ/mol per water molecule (Ladbury, 1996). If amiloride and benzamidine bind to MEC-4 channels in a similar manner as they do to urokinase, and binding amiloride displaces three additional H_2O molecules than binding benzamidine, then $\Delta\Delta G$ for binding should be in the range of 7–21 kJ/mol. Consistent with this idea, $\Delta\Delta G$ was −13.6 and −9.9 kJ/mol for A713wt and A713T channels, respectively. While this value is consistent with the binding model inferred from the urokinase structures, caution is warranted. Estimates of the entropic change generated by releasing bound water molecules are neither exact nor expected to be identical for all protein–ligand interactions.

We further propose that a water molecule is displaced from wild-type, A713V, and A713C channels when amiloride binds and that binding to the lower-affinity isoforms A713G, A713T, and A713D does not involve displacement of a water molecule. If this model is correct, then lower-affinity isoforms should exhibit similar free energies of binding or $\Delta G°$ at 0 mV and the difference in free energy between low and high-affinity isoforms ($\Delta\Delta G°$) should be ≤7 kJ/mol. Consistent with this idea, $\Delta\Delta G°$ for amiloride binding with respect to wild-type MEC-4 channels was ~2.75 kJ/mol on average (Table III). The $\Delta\Delta G°$ was larger for benzamil binding (−5.5 kJ/mol), but still <7 kJ/mol.

We note that the contribution of the *d* position to amiloride binding is modest especially when compared with effect of mutating other positions. For example, mutating the *d*+7 residue, which is either a glycine or a serine in most, if not all, wild-type channel subunits (see Fig. 1), in β or γ ENaC reduced amiloride affinity by ~1,000-fold (Schild et al., 1997). A less dramatic difference in affinity between αβ and αγ ENaC channels has been attributed to a 15-residue tract (*d*+1 to *d*+15) near the putative pore that differs between β and γ ENaC (McNicholas and Canessa, 1997). Differences in affinity between αβ and αγ ENaC channels cannot be attributed solely to *d*+7, however, since glycine occupies the *d*+7 position in both β and γ ENaC. These data are consistent with the idea that conserved glycines (and other small residues such as alanine and serine) play a structural role in folding the peptide backbone such that mutating these residues influences amiloride binding by altering the structure in this region of the channel.

The DEG/ENaC Channel Pore

As proposed by Palmer (1990) in an analysis of native ENaC channels, the general body plan of the outer pore of MEC-4 and other DEG/ENaC channels can be described as a funnel, wide enough to accommodate amiloride and benzamil on the extracellular side, but slim enough at the selectivity filter to discriminate between Na^+ and K^+. Our data are consistent with a model in which the *d* residue is near the rim of this funnel, positioned on the extracellular side of the putative selectivity filter. The following observations support this conclusion. First, the *d* residue is outside of the selectivity filter since the relative ion permeability was essentially wild type in all A713X isoforms (Table I). Second, the effect of mutation on sensitivity to amiloride and benzamil places the *d* residue on the extracellular side since both drugs act from the extracellular side. Modification of A713C channels by extracellular MTSES also supports this localization. Additional evidence comes from the observation that A713D had a significantly greater single-channel conductance than the other isoforms tested (Fig. 3 B). This result could reflect the ability of negatively charged residues to concentrate positively charged permeant ions and increase single-channel conductance (Green and Andersen, 1991). A similar effect could be responsible for the increase in macroscopic current amplitude elicited by extracellular application of MTSES to A713C channels, a manipulation that also introduces a negative charge at the *d* position. In agreement with the idea that side-chain charge at the *d* position affects single-channel conductance, modification by MTSET, which is positively charged, decreased the single-channel conductance of αβγENaC channels carrying a cysteine at the *d* position in the β subunit (Kellenberger et al., 2002).

We thank R.W. Aldrich for comments.

This work was supported by grants from American Heart Association (AHA) (Western States Affiliate), National Institute of Neurological Disorders and Stroke, Sloan Foundation, Donald B. and Delia E. Baxter Foundation, and Terman Fellowships to M.B. Goodman, and an AHA predoctoral fellowship (Western States Affiliate) to A.L. Brown.

Lawrence G. Palmer served as editor.

Submitted: 26 September 2006
Accepted: 3 January 2007

REFERENCES

Adams, C.M., P.M. Snyder, M.P. Price, and M.J. Welsh. 1998. Protons activate brain Na^+ channel 1 by inducing a conformational change that exposes a residue associated with neurodegeneration. *J. Biol. Chem.* 273:30204–30207.

Bass, R.B., P. Strop, M. Barclay, and D.C. Rees. 2002. Crystal structure of *Escherichia coli* MscS, a voltage-modulated and mechanosensitive channel. *Science.* 298:1582–1587.

Bateman, A., L. Coin, R. Durbin, R.D. Finn, V. Hollich, S. Griffiths-Jones, A. Khanna, M. Marshall, S. Moxon, E.L. Sonnhammer, et al. 2004. The Pfam protein families database. *Nucleic Acids Res.* 32:D138–D141.

Canessa, C.M., L. Schild, G. Buell, B. Thorens, I. Gautschi, J.D. Horisberger, and B.C. Rossier. 1994. Amiloride-sensitive epithelial Na^+ channel is made of three homologous subunits. *Nature.* 367:463–467.

Chalfie, M., and E. Wolinsky. 1990. The identification and suppression of inherited neurodegeneration in *Caenorhabditis elegans*. *Nature.* 345:410–416.

Chang, G., R.H. Spencer, A.T. Lee, M.T. Barclay, and D.C. Rees. 1998. Structure of the MscL homolog from *Mycobacterium tuberculosis*: a gated mechanosensitive ion channel. *Science.* 282:2220–2226.

Choudhary, G., M. Yotsu-Yamashita, L. Shang, T. Yasumoto, and S.C. Dudley Jr. 2003. Interactions of the C-11 hydroxyl of tetrodotoxin with the sodium channel outer vestibule. *Biophys. J.* 84:287–294.

Driscoll, M., and M. Chalfie. 1991. The *mec-4* gene is a member of a family of *Caenorhabditis elegans* genes that can mutate to induce neuronal degeneration. *Nature.* 349:588–593.

Garty, H., and L.G. Palmer. 1997. Epithelial sodium channels: function, structure, and regulation. *Physiol. Rev.* 77:359–396.

Gillespie, J.I. 1983. The distribution of small ions during the early development of *Xenopus laevis* and *Ambystoma mexicanum* embryos. *J. Physiol.* 344:359–377.

Goodman, M.B., G.G. Ernstrom, D.S. Chelur, R. O'Hagan, C.A. Yao, and M. Chalfie. 2002. MEC-2 regulates *C. elegans* DEG/ENaC channels needed for mechanosensation. *Nature.* 415:1039–1042.

Green, W.N., and O.S. Andersen. 1991. Surface charges and ion channel function. *Annu. Rev. Physiol.* 53:341–359.

Hidalgo, P., and R. MacKinnon. 1995. Revealing the architecture of a K^+ channel pore through mutant cycles with a peptide inhibitor. *Science.* 268:307–310.

Hille, B. 2001. Ion Channels of Excitable Membranes. Third edition. Sinauer Associates, Inc., Sunderland, MA. 814 pp.

Hong, K., I. Mano, and M. Driscoll. 2000. *In vivo* structure-function analyses of *Caenorhabditis elegans* MEC-4, a candidate mechanosensory ion channel subunit. *J. Neurosci.* 20:2575–2588.

Huang, M., and M. Chalfie. 1994. Gene interactions affecting mechanosensory transduction in *Caenorhabditis elegans*. *Nature.* 367:467–470.

Jones, M.V., Y. Sahara, J.A. Dzubay, and G.L. Westbrook. 1998. Defining affinity with the $GABA_A$ receptor. *J. Neurosci.* 18:8590–8604.

Kash, T.L., A. Jenkins, J.C. Kelley, J.R. Trudell, and N.L. Harrison. 2003. Coupling of agonist binding to channel gating in the GABA(A) receptor. *Nature.* 421:272–275.

Kellenberger, S., I. Gautschi, and L. Schild. 2002. An external site controls closing of the epithelial Na^+ channel ENaC. *J. Physiol.* 543:413–424.

Kellenberger, S., I. Gautschi, and L. Schild. 2003. Mutations in the epithelial Na^+ channel ENaC outer pore disrupt amiloride block by increasing its dissociation rate. *Mol. Pharmacol.* 64:848–856.

Kellenberger, S., and L. Schild. 2002. Epithelial sodium channel/degenerin family of ion channels: a variety of functions for a shared structure. *Physiol. Rev.* 82:735–767.

Ladbury, J.E. 1996. Just add water! The effect of water on the specificity of protein-ligand binding sites and its potential application to drug design. *Chem. Biol.* 3:973–980.

Lai, C.-C., K. Hong, M. Kinnell, M. Chalfie, and M. Driscoll. 1996. Sequence and transmembrane topology of MEC-4, an ion channel subunit required for mechanotransduction in *Caenorhabditis elegans*. *J. Cell Biol.* 133:1071–1081.

McNicholas, C.M., and C.M. Canessa. 1997. Diversity of channels generated by different combinations of epithelial sodium channel subunits. *J. Gen. Physiol.* 109:681–692.

O'Hagan, R., M. Chalfie, and M.B. Goodman. 2005. The MEC-4 DEG/ENaC channel of *Caenorhabditis elegans* touch receptor neurons transduces mechanical signals. *Nat. Neurosci.* 8:43–50.

Palmer, L.G. 1990. Epithelial Na channels: the nature of the conducting pore. *Ren. Physiol. Biochem.* 13:51–58.

Palmer, L.G., and G. Frindt. 1986. Amiloride-sensitive Na channels from the apical membrane of the rat cortical collecting tubule. *Proc. Natl. Acad. Sci. USA.* 83:2767–2770.

Rabito, C.A., C.A. Rotunno, and M. Cereijido. 1978. Amiloride and calcium effect on the outer barrier of the frog skin. *J. Membr. Biol.* 42:169–187.

Royal, D.C., L. Bianchi, M.A. Royal, M. Lizzio Jr., G. Mukherjee, Y.O. Nunez, and M. Driscoll. 2005. Temperature-sensitive mutant of the *Caenorhabditis elegans* neurotoxic MEC-4(d) DEG/ENaC channel identifies a site required for trafficking or surface maintenance. *J. Biol. Chem.* 280:41976–41986.

Schild, L., E. Schneeberger, I. Gautschi, and D. Firsov. 1997. Identification of amino acid residues in the α, β, and γ subunits of the epithelial sodium channel (ENaC) involved in amiloride block and ion permeation. *J. Gen. Physiol.* 109:15–26.

Schreiber, G., and A.R. Fersht. 1995. Energetics of protein-protein interactions: analysis of the barnase-barstar interface by single mutations and double mutant cycles. *J. Mol. Biol.* 248:478–486.

Snyder, P.M., D.B. Bucher, and D.R. Olson. 2000. Gating induces a conformational change in the outer vestibule of ENaC. *J. Gen. Physiol.* 116:781–790.

Vassalli, J.D., and D. Belin. 1987. Amiloride selectively inhibits the urokinase-type plasminogen activator. *FEBS Lett.* 214:187–191.

Woodhull, A.M. 1973. Ionic blockage of sodium channels in nerve. *J. Gen. Physiol.* 61:687–708.

Zeslawska, E., A. Schweinitz, A. Karcher, P. Sondermann, S. Sperl, J. Sturzebecher, and U. Jacob. 2000. Crystals of the urokinase type plasminogen activator variant βc-uPA in complex with small molecule inhibitors open the way towards structure-based drug design. *J. Mol. Biol.* 301:465–475.